Modulation of terahertz-spectrum generation from an air plasma by tunable three-color laser pulses

Chenhui Lu,[1,*] Chunyan Zhang,[1] Liqiang Zhang,[1] Xianwei Wang,[2] and Shian Zhang[3,†]

[1]*College of Mechanical Engineering, Shanghai University of Engineering Science, Shanghai 201620, People's Republic of China*

[2]*College of Science, Zhejiang University of Technology, Hangzhou, Zhejiang 310023, People's Republic of China*

[3]*State Key Laboratory of Precision Spectroscopy and School of Physics and Materials Science, East China Normal University, Shanghai 200062, People's Republic of China*

(Received 27 February 2017; published 6 November 2017)

We theoretically demonstrate that the terahertz-spectrum generation in three-color laser-gas interactions can be effectively manipulated by tuning the laser wavelengths. We show that by positive and negative detuning of one of the color laser wavelengths in the three-color laser pulse, the terahertz spectral range can be greatly expanded, and in particular, the high spectral frequency components emerge. However, the total terahertz energy is maintained at a relatively high level and can even significantly increase. Moreover, we also show that the middle and high spectral frequency components of the terahertz spectrum can be effectively tuned by modulating the relative wavelength of the three-color laser pulses. Finally, our analysis shows that the ionization events play an important role in the intense and shaped terahertz generation.

DOI: 10.1103/PhysRevA.96.053402

I. INTRODUCTION

Terahertz (THz) generation from laser-induced plasmas has attracted considerable attention for the capabilities of obtaining intense and broadband THz radiation, which are extremely important for various related fields in molecular physics, material sciences, and biological-medical imaging [1–5]. In this THz generation scheme, a one-color femtosecond laser pulse (usually with a wavelength near 800 nm from a Ti:sapphire generator) combines with its second-harmonic field to ionize the ambient air. Then the produced free electrons are simultaneously accelerated by this incommensurate field and form the directional electron current, which finally results in intense THz radiation [6–9]. The two-color scheme has been well studied in theory and experiment, and it has been demonstrated that the symmetry breaking of the laser pulse plays a key role in this process [10–20]. Thus, to further enhance the intensity and bandwidth of the THz pulse, the construction of an incommensurate laser field is particularly important. With further study of the scheme, some studies experimentally show that a near-IR and even far-IR laser pulse can further enhance the THz radiation intensity [21,22]. The role of the increased fundamental wavelength has also been theoretically analyzed in this phenomenon [23]. It is natural to assume that more color lasers can be applied to construct the asymmetric laser fields and generate the intense THz radiation.

A recent study by Martinez *et al.* demonstrated that the multiple-harmonic laser pulse can effectively optimize the free electron trajectories and improve the THz conversion efficiency [24]. In their method, the standard three or more harmonic fields of the near-IR laser pulse have been used to construct the incommensurate field and enhance the THz radiation. Furthermore, the latest work shows that the electron excitation for THz generation can be attributed to the ionization-induced multiwave mixing, and the nonharmonic frequency ratios can also be used to compose the ionizing two-color laser pulse [25]. Thus it is of interest to further study the THz generation with incomplete multiple-harmonic laser pulses. This is because most of the laser pulse wavelengths are fixed to construct the asymmetric laser fields, and the other laser pulse wavelengths can be mixed to adjust the THz intensity and spectrum.

In this paper, we theoretically study THz generation with nonharmonic three-color laser pulses based on a transient photocurrent model. Our results show that the THz spectrum can be greatly expanded and effectively modulated by frequency detuning the three-color laser wavelengths. With this approach, the high spectral frequency components emerge in the THz spectrum, while the low spectral frequency components are suppressed, which greatly changes the THz spectral shape. However, the THz yield maintains at a relative high level and can significantly increase for the negative detuning of the shortest wavelength and positive detuning of the longest wavelength of the nonharmonic three-color laser pulse. Furthermore, it is also shown that the middle and high spectral frequency components of the THz spectrum can be effectively modulated by detuning one color laser wavelength of the nonharmonic three-color laser pulses. Finally, we utilize the local current (LC) model to illustrate the physical mechanism of the THz spectral modulation and radiation enhancement.

II. THEORETICAL MODEL

Our theoretical simulation is based on the transient photocurrent model [8,11,14,15,17,18,24,26]. The generally employed standard three-color laser field is a superposition of the fundamental laser field and its second- and third-harmonic laser fields, which can be expressed as

$$E(t) = \exp(-2\ln 2t^2/\tau^2)[E_1\cos(\omega_0 t+\phi_1) + E_2\cos(2\omega_0 t+\phi_2)+E_3\cos(3\omega_0 t+\phi_3)], \quad (1)$$

where E_1, E_2, and E_3 are, respectively, the field amplitude of the fundamental, second-, and third-harmonic laser field; τ is the pulse duration, ω_0 is the central frequency of the fundamental laser field; and ϕ_1, ϕ_2, and ϕ_3 are the relative

*lchhuiz@163.com

†sazhang@phy.ecnu.edu.cn

phases of the three-color laser pulse. The main parameters in this standard three-harmonic laser pulse are usually set to $E_1 = 2E_2 = 3E_3$ and $\phi_2 = -\phi_1 = -\phi_3 = \pi/2$, which has been shown to optimize the electron trajectory and enhance the THz radiation intensity [24]. In our simulation, the central frequency of the fundamental laser field is set to $\omega_0 =$ 187.5 THz, corresponding to the wavelength $\lambda_0 = 1600$ nm, since more harmonics can be accessible in practice. We focus on the effect of the laser detuning wavelength on the THz generation, and thus the main parameters were fixed so that only one-color laser wavelength is variable. Here $\delta\omega_1$, $\delta\omega_2$, and $\delta\omega_3$ represent the detuning frequencies of the three laser pulses. For the intensity regime of our simulation ($10^{14} - 10^{15}$ W/cm^2), the Keldysh parameter is $\gamma \leqslant 1$ and the tunneling ionization is the dominant ionization route. The ionization ratio can be calculated with either the static tunneling (ST) model [27,28] or the Ammosov-Delone-Krainov (ADK) model [29,30]. Here, the well-known static tunneling model is employed, and the ionization rate can be expressed by

$$W_{\rm st} = \frac{\alpha_{\rm ST}}{|\varepsilon(t)|} \exp\left\{-\left[\frac{\beta_{\rm ST}}{\varepsilon(t)}\right]\right\}, \tag{2}$$

where $\varepsilon(t) = E(t)/\varepsilon_a$, ε_a is the electric field in atomic units, $\alpha_{\rm ST} = 4\omega_a r_{\rm H}^{5/2}$, $\beta_{\rm ST} = (2/3)r_{\rm H}^{3/2}$, ω_a is the atomic frequency unit with $\omega_a = \kappa^2 m e^4/\hbar^3 \approx 4.13 \times 10^{16}\,{\rm s}^{-1}$, and $r_{\rm H}$ is the ionization potential of the gas molecule relative to the hydrogen atom $r_{\rm H} = U_{\rm ion}/U_{\rm ion}^{\rm H}$. In our simulation, we use $U_{\rm ion} = 15.6$ eV (for N_2 gas) and $U_{\rm ion}^{\rm H} = 13.6$ eV. Given the ionization rate $W_{\rm st}$, the increasing rate of the electron density can be expressed by

$$\frac{dN_e(t)}{dt} = W_{\rm st}[N_g - N_e(t)], \tag{3}$$

where $N_e(t)$ is the time-dependent electron density and N_g is the initial neutral gas density. We use the final ionization degree $W_{\rm fi}$ as a measurement of the electron density, which is given by

$$W_{\rm fi} = N_e(t = \infty)/N_g. \tag{4}$$

For complete ionization, $W_{\rm fi} = 1$. In our simulation, the amplitude of the fundamental laser pulse E_1 is set to produce a moderate ionization degree $W_{\rm fi} = 0.4$ at the standard three-color pulse, since the effects of the laser parameters will be different at higher laser intensities [31,32]. Once freed from the parent molecule, the electron will oscillate with the laser field, and the electron velocity at a subsequent time can be written as

$$v(t,t') = -\frac{e}{m}\int_{t'}^{t} dt'' E(t''), \tag{5}$$

where t' is the ionization instant. Considering the contribution of all ionized electrons, the generated transverse electron current can be expressed by

$$J(t) = \int_{-\infty}^{t} ev(t,t') \exp[-\gamma(t - t')] dN_e(t'), \tag{6}$$

where $dN_e(t')$ represents the change of the electron density in the interval between t' and $t'+dt'$, $v(t,t')$ can be seen as the velocity of an electron born at $-\infty$ that undergoes variations at the ionization instant t' of the pulse (which denotes the electron drift velocity), and γ is the phenomenological electron-ion collision rate ($\gamma \cong 5\,{\rm ps}^{-1}$ at atmospheric pressure) [26]. The time-dependent electron current $J(t)$ can generate an electromagnetic pulse at THz frequencies in the far field. The amplitude of the generated THz field is proportional to the derivative of the electron current $J(t)$ and is written as

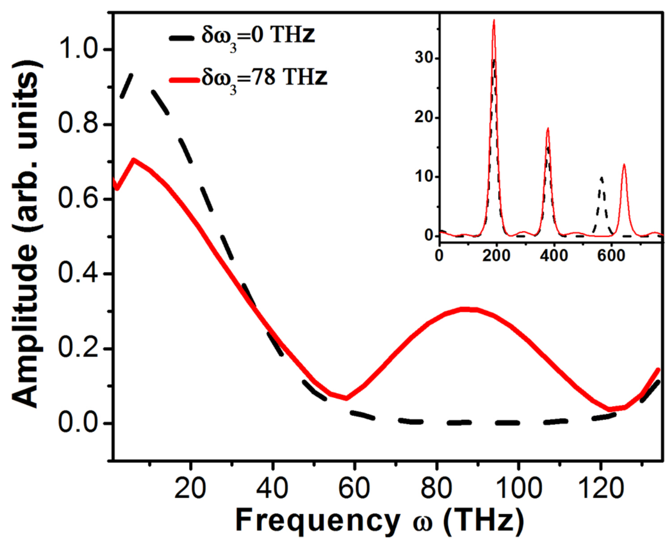

FIG. 1. The THz radiation spectrum for the harmonic (black dashed line) and nonharmonic three-color laser pulse with a detuning frequency of $\delta\omega_3 = 78$ THz (red solid line). The inset shows the corresponding radiative electromagnetic spectrum for the two cases.

$$E_{\rm THz} \propto \frac{d}{dt}[J(t)]. \tag{7}$$

Finally, the THz radiation spectrum is obtained by the Fourier transform of $E_{\rm THz}(t)$; i.e., $E_{\rm THz}(\omega) = {\rm FFT}[E_{\rm THz}(t)]$.

III. RESULTS AND DISCUSSION

In this work, we first demonstrate the modulation of a nonharmonic three-color laser pulse on the THz spectrum, and the corresponding change in the radiative electromagnetic spectrum. Figure 1 shows the THz radiation spectrum with the harmonic (black dashed line) and nonharmonic (red solid line) three-color laser pulse. As seen, the THz radiation is generated up to ~100 THz for the nonharmonic three-color laser pulse, and the high spectral frequency components emerge in the THz spectral range and reach a moderate intensity. The resulting radiative electromagnetic spectrum is also modulated by the incommensurate laser pulse, as seen in the inset of Fig. 1. The more spectral frequency components emerge in the radiative electromagnetic spectrum and surround the pump laser frequency components for the nonharmonic three-color laser pulse. Since the near-IR pump laser frequency components are close to the THz spectral range, these frequency satellites produced upon the multiwave mixing can significantly alter the THz spectral shape at more high-frequency components. Furthermore, it is worth noting that the amplitude of the low-frequency THz radiation and the total THz yield do not significantly decrease, which is different from THz radiation for the similar positive detuning of the second harmonic in the incommensurate two-color

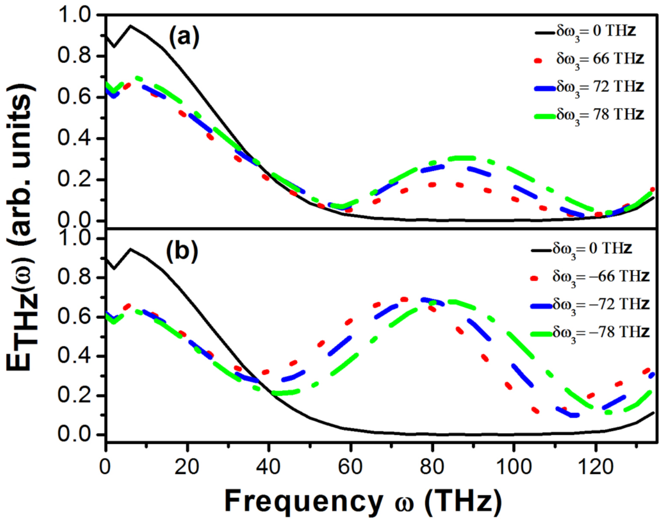

FIG. 2. (a) The THz spectrum for the nonharmonic three-color laser pulse with a positive detuning frequency of $\delta\omega_3 = 0$ (black solid line), 66 (red dotted line), 72 (blue dashed line), and 78 (green dash-dotted line) THz. (b) The THz spectrum with a negative detuning for the four cases.

laser [26,33]. In that case (especially in the latter reference), since the second harmonic causes a bigger group delay with respect to the fundamental pulse for the positive detuning, the asymmetry of the laser pulse is dramatically destroyed. Thus most of the ionization electrons cannot obtain a large drift velocity, which consequently cancels out the net current and suppresses the THz radiation. For the nonharmonic three-color lasers, the two harmonic laser pulses basically maintain the drift movement of most ionization electrons so that the amplitude of the net current will not significantly decrease. Therefore, the other laser pulse can be mixed to further affect the ionization process and modulate the THz spectrum.

Next, we specifically study THz generation for the nonharmonic three-color laser pulse by individual varying the one-color laser wavelength. Figure 2(a) shows the THz spectrum for the nonharmonic three laser pulse by positively detuning the shortest wavelength laser pulse with the detuning frequency of $\delta\omega_3 = 0$ (black solid line), 66 (red dotted line), 72 (blue dashed line), and 78 (green dash-dotted line) THz. As seen, the amplitude of the THz spectrum decreases by approximately 30% for the positive detuning, and the high spectral frequency components emerge in the THz spectral range. The total THz yield does not significantly decrease with the further increase of the high spectral component intensity. It can also be seen that the amplitude and central position of the high spectral frequency components are enhanced with the increase of the detuning frequency $\delta\omega_3$. Figure 2(b) also shows the THz generation with negative detuning of the shortest wavelength laser pulse. As seen, by comparing the results of Fig. 2(a), in which the amplitudes of high-frequency components are relatively low, this amplitude further increases and is even higher than the amplitude of low-frequency components for the negative detuning. Therefore, the total THz yield apparently increases. Moreover, the peak position of the high-frequency components can be effectively adjusted. It is noteworthy that the positive and negative detuning can both effectively alter the THz spectral shape. In addition, the THz radiation intensity does not significantly decrease for the positive detuning, which differs from the cases for an incommensurate two-color laser [26,33]. Thus the nonharmonic three-color laser scheme can be regarded as an alternatively shaped THz pulse generation method in addition to the two-color setup.

To illustrate the physical mechanism of spectral modulation, the analysis approach proposed by Babushkin *et al.* [26] is introduced in our discussion. In this model, the THz radiation is attributed to the contribution of discrete ionization events, which provides a treatment at the microscopic level for understanding the THz generation process. Specifically, the free electron density $\rho(t)$ is considered to increase during the short attosecond-scale ionization events that only occur near the extreme of the laser field at times t_n. Each ionization event is well separated from the others, and has well-defined amplitude $\delta\rho_n$ and shape $H_n(t)$. Therefore, the electron density can be written as a discrete sum,

$$\rho(t) = \sum_n \delta\rho_n H(t - t_n), \tag{8}$$

where H is a "smoothed" step function. Taking into account the electron velocity, the electron current can be written as a sum of these separated attosecond currents,

$$J(t) = \sum_n J_n(t) = \sum_n q\delta\rho_n H(t - t_n)[v_f(t) - v_f(t_n)], \tag{9}$$

where $v_f(t) = \frac{q}{m}\int_{-\infty}^{t} E(\tau)d\tau$ and q are the free electron velocity and electron charge, respectively. In the LC limit, the generated THz pulse in the frequency domain can be obtained by the Fourier transform of Eq. (9) (neglecting the slowly varying and pump items):

$$E_{\mathrm{THz}}(\omega) \propto \sum_n C_n e^{i\omega t_n}, \tag{10}$$

with

$$C_n = q\delta\rho_n v_f(t_n), \tag{11}$$

where C_n is the amplitude of the nth attosecond current burst that is localized near the nth ionization events, and $\delta\rho_n$ and $v_f(t_n)$, respectively, represent the electron density and velocity for the nth ionization event. As seen in Eq. (10), the THz spectrum is a superposition of contributions from these individual ionization events with a structure that is mainly determined by interference due to the spectral phases $e^{i\omega t_n}$. This alternative approach provides a relatively easy prediction of the THz amplitude and spectral structure for arbitrary input field shapes, which is useful to analyze our results. For the standard three-harmonic laser pulse, these contributions cancel each other at high frequencies and interfere constructively at low frequencies, and thus the typical THz spectral structure can be obtained which is similar to that for the two-color laser pulse irradiation [26]. However, the interference will be different for the nonharmonic three-color laser pulse.

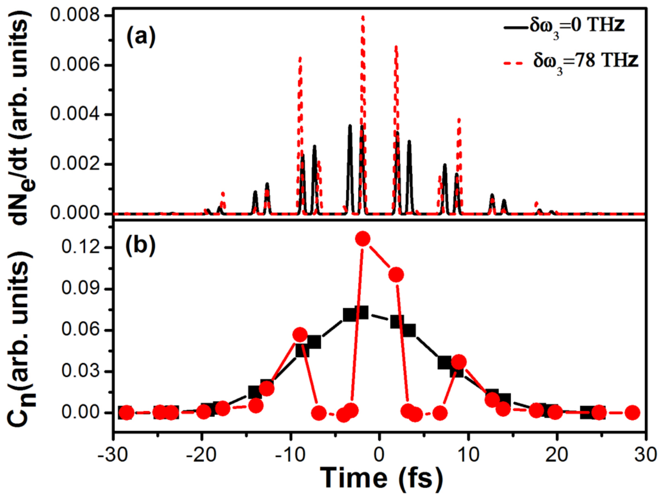

FIG. 3. (a) The increasing rate of the electron density $dN_e(t)/dt$ for the harmonic (black solid line) and nonharmonic three-color laser pulse with a detuning frequency of $\delta\omega_3 = 78$ THz (red dashed line). (b) The corresponding amplitude of nth current bursts C_n for the harmonic (black squares) and nonharmonic (red circles) three-color laser pulse.

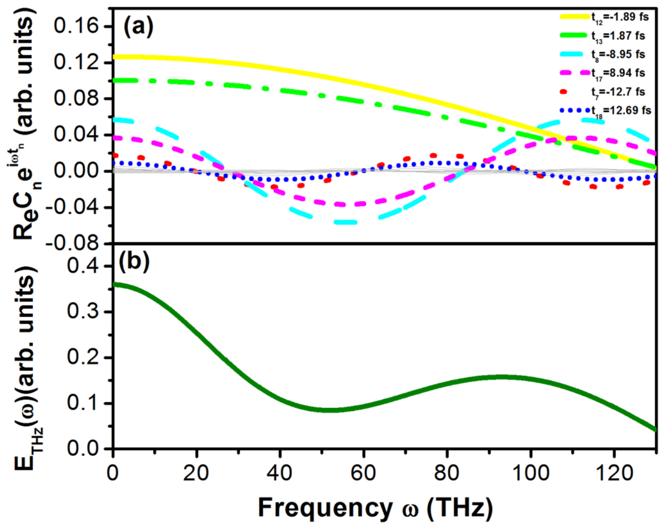

FIG. 4. (a) The contributions of nth ionization events $R_e C_n e^{i\omega t_n}$ and (b) the resulting THz spectrum $E_{\mathrm{THz}}(\omega)$ for the nonharmonic three-color laser pulse with a detuning frequency of $\delta\omega_3 = 78$ THz. The color lines of the main contributions are deepened, and the corresponding ionization times are given in the legend.

Figure 3(a) shows the increasing rate of the electron density $dN_e(t)/dt$ for the standard three-color laser pulse (black solid line) and nonharmonic three-color laser pulse with a detuning frequency of $\delta\omega_3 = 78$ THz (red dashed line). As seen, the ionization event is distributed on both sides of the laser center and only occurs near the extreme of the laser field. For the standard three-color laser pulse, the ionization events appear in pairs, and the adjacent events show similar ionization rates, which means that the electron density $\delta\rho_n$ of the two adjacent ionization events are close to each other. However, for the nonharmonic three-color laser pulse, the ionization rates of adjacent ionization events are significantly different, where one is suppressed but the other is markedly increased. Therefore, the electron generation is concentrated in a few ionization events, and a single ionization event will produce more electrons. Figure 3(b) further shows the amplitude of the nth current bursts C_n for the harmonic (black squares) and nonharmonic (red circles) three-color laser pulses. As seen, the distribution of the ionization events is associated with the ionization process, and their amplitudes mainly depend on the electron density $\delta\rho_n$ for frequency detuning. It is noteworthy that the amplitudes of the six ionization events that only occur near the center of the laser pulse reach high values for the nonharmonic laser pulse and will significantly alter the THz spectral structure.

Figure 4 shows the contributions of nth ionization events $R_e C_n e^{i\omega t_n}$ [Fig. 4(a)] and the resulting THz spectrum $E_{\mathrm{THz}}(\omega)$ [Fig. 4(b)] for the nonharmonic three-color laser pulse with a detuning frequency of $\delta\omega_3 = 78$ THz. As seen in Fig. 4(a), the main ionization events acquire a high amplitude, and their contributions constructively interfere at low frequencies, so that the typical THz spectral structure can be obtained in the low-frequency range, which is similar to the situation for the standard two-color [26] or three-color laser pulse irradiation. However, the effect of destructive interference is not obvious at high frequencies, and the contributions still show distinctly constructive interference properties at the high-frequency range. Therefore, the more frequency components emerge in the THz spectrum, which is contrary to the situation of the standard three-color laser pulse in which the contributions cancel each other, and no THz spectrum emerges in the high-frequency range. In other words, since the electron generation is concentrated near the center of the laser pulse, a single ionization event obtains the high amplitude, and its contribution is slowly varied. The few occurring ionization events are not symmetrically distributed; thus the total contributions provide more constructive interference in the high-frequency THz range, which ultimately alters the THz spectral structure and results in the emergence of the high-frequency component. The theoretical analysis agrees well with our results, and the remaining cases of frequency detuning can also be explained by the model in a similar way.

Figure 5(a) shows the THz spectrum for the nonharmonic three-color laser pulse by positively detuning the middle wavelength laser pulse with a detuning frequency of $\delta\omega_2 = 45$ (blue solid line), 48 (red dashed line), and 51 (black dotted line) THz. As seen, the positive detuning significantly alters the THz spectral shape. The low-frequency THz radiation is effectively suppressed, and two distinct spectral peaks emerge in the middle- and high-THz spectral range. Furthermore, the central frequency of the middle and high spectral frequency components can be effectively detuned by varying the middle wavelength laser pulse. Then the peak position of the middle-frequency and high-frequency spectra, respectively, decrease and increase as the detuning frequency $\delta\omega_2$ decreases. Figure 5(b) also shows the THz spectrum with negative detuning of the middle wavelength laser pulse. It is interesting that the THz spectra exhibit the same modulation characteristics.

We also present the THz spectrum for the nonharmonic three-color laser pulse by positively detuning the longest

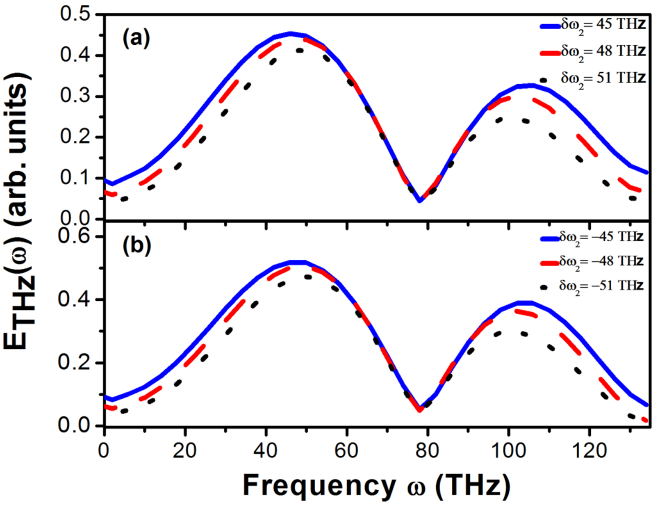

FIG. 5. (a) The THz spectrum for the nonharmonic three-color laser pulse with a positive detuning frequency of $\delta\omega_2 = 45$ (blue solid line), 48 (red dashed line), and 51 (black dotted line) THz. (b) The THz spectrum with a negative detuning for the three cases.

wavelength laser pulse with a detuning frequency of $\delta\omega_1 = 24$ (black dotted line), 27 (red dashed line), and 30 (blue solid line) THz, as shown in Fig. 6. One can see that the low-frequency THz radiation is suppressed, and a single peak with a broad bandwidth appears in the THz spectral range. Furthermore, the spectral peak shifts with the increase of the detuning frequency $\delta\omega_1$, and the THz spectrum can be tuned over a wider spectral range. However, the negative detuning does not alter the THz spectral shape, but dramatically suppresses the THz radiation since the high-frequency components have been mixed in the shortest pump spectral range, as seen in the inset of

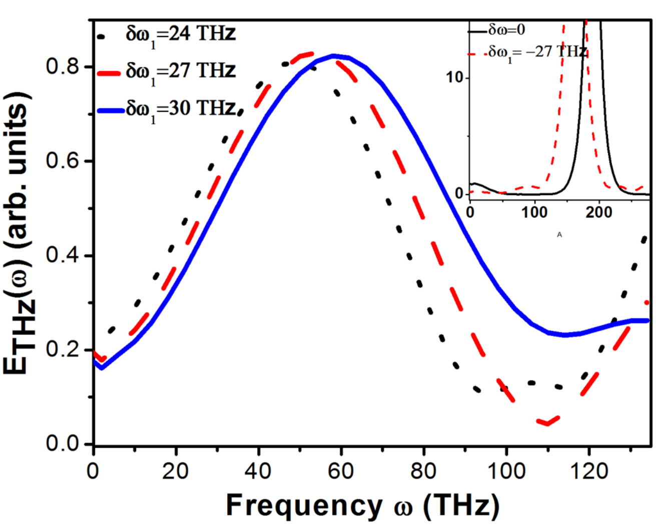

FIG. 6. The THz spectrum for the nonharmonic three-color laser pulse with a positive detuning frequency of $\delta\omega_1 = 24$ (black dotted line), 27 (red dashed line), and 30 THz (blue solid line). The inset shows the electromagnetic spectrum around the shortest pump spectral range for the harmonic (black solid line) and nonharmonic three-color laser pulse with a negative detuning frequency of $\delta\omega_1 = -27$ THz (red dashed line).

TABLE I. The THz energy U_{THz} and the corresponding finial ionization degree W_{fi} with a detuning frequency of $\delta\omega$ for the nonharmonic three-color laser pulse in our simulation. Here, the ionization degree and THz energy are normalized to the harmonic three-color pulse. The cases of THz yield enhancement are highlighted inside the bold lines.

$\delta\omega_3$	W_{fi}	U_{THz}	$\delta\omega_3$	W_{fi}	U_{THz}	$\delta\omega_2$	W_{fi}	U_{THz}
66	1.21	0.56	−66	1.21	1.29	45	0.64	0.45
72	1.21	0.64	−72	1.21	1.26	48	0.64	0.39
78	1.22	0.74	−78	1.23	1.23	51	0.63	0.31
$\delta\omega_2$	W_{fi}	U_{THz}	$\delta\omega_1$	W_{fi}	U_{THz}			
−45	0.64	0.59	24	1.59	1.29			
−48	0.64	0.52	27	1.55	1.39			
−51	0.64	0.41	39	1.51	1.55			

Fig. 6. As a result, these situations are not considered in detail here. The spectrum modulation with frequency detuning of the longest wavelength laser pulse is similar to the case for the incommensurate two-color laser irradiation, but the positive or negative sign of the frequency detuning are different for the two cases [26,33].

Finally, to further illustrate the effect of a nonharmonic three-color laser pulse on THz generation, we compared the terahertz energy $U_{\mathrm{THz}} \propto \int_0^{\omega_{\mathrm{co}}} E^2(\omega)d\omega$ and the corresponding final ionization degree W_{fi} for all frequency detuning situations in our simulation, as seen in Table I. Here, the cutoff frequency is chosen to be $\omega_{\mathrm{co}} = 120$ THz and the pump energy $a_1^2E_1^2 + a_2^2E_2^2 + a_3^2E_3^2$ is strictly fixed. One can see that the frequency detuning can effectively modulate the electron density. The final ionization degree decreases for both positive detuning and negative detuning of the middle wavelength laser pulse. This is because the 1600-nm fundamental pulse and the 533-nm third harmonic are fixed, making it difficult to construct the incommensurate structure compared to the other frequency ratio laser combinations [25], and the THz yield decreases with the decrease of the electron density. In the other three cases, the electron densities all significantly increase with frequency detuning, and the THz energy increases for negative detuning of the shortest wavelength and positive detuning of the longest wavelength. Nevertheless, the comparison of the final electron density is not sufficient to completely illustrate the modulation effects of the nonharmonic three-color laser pulse, since we find that the electron density reaches a high value while the THz yield decreases for positive detuning of the shortest wavelength. Thus the physical mechanism of the THz radiation enhancement is further discussed. Figure 7 shows the increasing rate of the electron density $dN_e(t)/dt$ for the three detuning cases. As seen, although the final electron densities are the same for a detuning frequency of $\delta\omega_3 = 72$ and -72 THz, the negative detuning concentrates the electron production in the two main ionization events. Thus the single ionization event obtains a higher amplitude, which results in intense THz radiation. One can also see that the main three ionization events can be further increased for a detuning frequency of $\delta\omega_1 = 27$ THz, providing the maximal THz yield. In general, the nonharmonic three-color setup can effectively

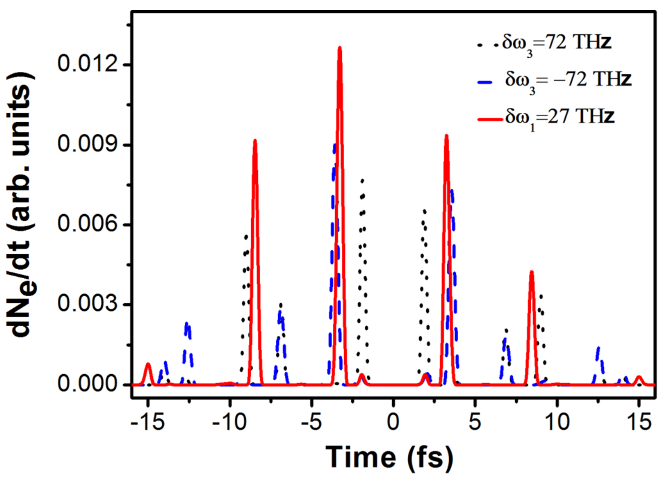

FIG. 7. The increasing rate of electron density $dN_e(t)/dt$ for the nonharmonic three-color laser pulse with a detuning frequency of $\delta\omega_3 = 72$ (black dotted line), $\delta\omega_3 = -72$ (blue dashed line), and $\delta\omega_1 = 27$ (red solid line) THz.

modulate the electron production and essentially maintains the ionized electron velocity. These properties ultimately determine the amplitude and distribution of the ionization events which result in the shaped and intense THz generation. These results further indicate that the tunneling ionization process plays an important role in the THz generation, and the nonharmonic three-color laser scheme can be used as an alternative approach to enhance the THz radiation.

In this paper, our simulations are based on the transient photocurrent model and focus on the microscopic effects of the nonharmonic three-color laser field on the electron current generation and the corresponding THz radiation spectrum. If the macroscopic propagation effect is further taken into account, the only difference is that the low-frequency THz radiation will not be completely suppressed for the result of Figs. 5 and 6 [26], since the forming and long-standing plasma permanently contributes toward the low-frequency THz radiation [34]. However, the modulation effect of the nonharmonic laser pulse on the THz spectrum will not significantly change [26,33]. Thus we are confident that the nonharmonic three-color laser pulse can also be used to modulate the terahertz spectrum.

IV. CONCLUSIONS

In conclusion, we have theoretically studied THz generation with a nonharmonic three-color laser pulse. Our results show that the THz spectrum can be effectively modulated, and the more spectral frequency components emerge in the THz spectral range. In addition, the middle and high spectral frequency components of the THz spectrum can be effectively detuned by individually varying the wavelength of a single color in the laser pulse. It was also shown that the THz energy is maintaind at a relatively high level and even significantly increases with frequency detuning. Finally, we utilized the LC model to explain the physical mechanism of the THz modulation and enhancement. The analysis shows that the nonharmonic setup can effectively control the distribution and amplitude of the ionization events, which results in the intense and shaped THz pulse generation. We believe that these theoretical results can serve as a basis for further experimental studies, and are also expected to be applied in various related fields.

ACKNOWLEDGMENTS

This work was partly supported by the National Natural Science Foundation of China (Grant No. 11604205), the Science and Technology Commission of Shanghai Municipality (Grant No. 14JC1401500), the Shanghai Municipal Education Commission (Grant No. ZZGCD15066), and the Zhejiang Provincial Natural Science Foundation (Grant No. LY17B030008).

[1] W. L. Chan, J. Deibel, and D. M. Mittleman, Imaging with terahertz radiation, Rep. Prog. Phys. **70**, 1325 (2007).
[2] M. C. Hoffman and J. A. Fülöp, Intense ultrashort terahertz pulse: Generation and applications, J. Phys. D **44**, 083001 (2001).
[3] E. Knoesel, M. Bonn, J. Shan, and T. F. Heinz, Charge Transport and Carrier Dynamics in Liquids Probed by THz Time-Domain Spectroscopy, Phys. Rev. Lett. **86**, 340 (2001).
[4] M. Woerner, W. Kuehn, P. Bowlan, K. Reimann, and T. Elsaesser, Ultrafast two-dimensional terahertz spectroscopy of elementary excitations in solids, New J. Phys. **15**, 025039 (2013).
[5] E. Pickwee and V. P. Wallace, Biomedical applications of terahertz technology, J. Phys. D **39**, R301 (2006).
[6] D. J. Cook and R. M. Hochstrasser, Intense terahertz pulses by four-wave rectification in air, Opt. Lett. **25**, 1210 (2000).
[7] M. Kress, T. Löffler, S. Eden, M. Thomson, and H. G. Roskos, Terahertz-pulse generation by photoionization of air with laser pulses composed of both fundamental and second-harmonic waves, Opt. Lett. **29**, 1120 (2004).
[8] H. G. Roskos, M. D. Thomson, M. Kreß, and T. Löffler, Broadband THz emission from gas plasmas induced by femtosecond optical pulses: From fundamentals to applications, Laser Photonics Rev. **1**, 349 (2007).
[9] K. Y. Kim, A. J. Taylor, J. H. Glownia, and G. Rodriguez, Coherent control of terahertz supercontinuum generation in ultrafast laser–gas interactions, Nat. Photonics **2**, 605 (2008).
[10] X. Xie, J. Dai, and X.-C. Zhang, Coherent Control of THz Wave Generation in Ambient Air, Phys. Rev. Lett. **96**, 075005 (2006).
[11] K. Y. Kim, J. H. Glownia, A. J. Taylor, and G. Rodriguez, Terahertz emission from ultrafast ionizing air in symmetry-broken laser fields, Opt. Express **15**, 4577 (2007).
[12] V. B. Gildenburg and N. V. Vvedenskii, Optical-to-THz Wave Conversion via Excitation of Plasma Oscillations in the Tunneling-Ionization Process, Phys. Rev. Lett. **98**, 245002 (2007).

[13] A. A. Silaev and N. V. Vvedenskii, Residual-Current Excitation in Plasmas Produced by Few-Cycle Laser Pulse, Phys. Rev. Lett. **102**, 115005 (2009).

[14] I. Babushkin, W. Kuehn, C. Köhler, S. Skupin, L. Bergé, K. Reimann, M. Woerner, J. Herrmann, and T. Elsaesser, Ultrafast Spatiotemporal Dynamics of Terahertz Generation by Ionizing Two-Color Femtosecond Pulses in Gases, Phys. Rev. Lett. **105**, 053903 (2010).

[15] L. Bergé, S. Skupin, C. Köhler, I. Babushkin, and J. Herrmann, 3D Numerical Simulation of THz Generation by Two-Color Laser Filaments, Phys. Rev. Lett. **110**, 073901 (2013).

[16] N. Karpowicz, X. Lu, and X.-C. Zhang, Terahertz gas photonics, J. Mod. Opt. **56**, 1137 (2009).

[17] K. Y. Kim, Generation of coherent terahertz radiation in ultrafast laser-gas interactions, Phys. Plasmas **16**, 056706 (2009).

[18] T. I. Oh, Y. S. You, N. Jhajj, E. W. Rosenthal, H. M. Milchberg, and K. Y. Kim, Intense terahertz generation in two-color laser filamentation: Energy scaling with terawatt laser systems, New J. Phys. **15**, 075002 (2013).

[19] H.-C. Wu, J. Meyer-ter-Vehn, and Z.-H. Sheng, Phase-sensitive terahertz emission from gas targets irradiated by few-cycle laser pulses, New J. Phys. **10**, 043001 (2008).

[20] D. Zhang, Z. Lü, C. Meng, X. Du, Z. Zhou, Z. Zhao, and J. Yuan, Synchronizing Terahertz Wave Generation with Attosecond Bursts, Phys. Rev. Lett. **109**, 243002 (2012).

[21] M. Clerici, M. Peccianti, B. E. Schmidt, L. Caspani, M. Shalaby, M. Giguère, A. Lotti, A. Couairon, F. Légaré, T. Ozaki, D. Faccio, and R. Morandotti, Wavelength Scaling of Terahertz Generation by Gas Ionization, Phys. Rev. Lett. **110**, 253901 (2013).

[22] N. V. Vvedenskii, A. I. Korytin, V. A. Kostin, A. A. Murzanev, A. A. Silaev, and A. N. Stepanov, Two-Color Laser-Plasma Generation of Terahertz Radiation Using a Frequency-Tunable Half Harmonic of a Femtosecond Pulse, Phys. Rev. Lett. **112**, 055004 (2014).

[23] A. Nguyen, P. González de Alaiza Martinez, J. Déchard, I. Thiele, I. Babushkin, S. Skupin, and L. Bergé, Spectral dynamic of THz pulses generated by two-color laser filaments in air: The role of Kerr nonlinearities and pump wavelength, Opt. Express **25**, 4720 (2017).

[24] P. G. Martinez, I. Babushkin, L. Bergé, S. Skupin, E. Cabrera-Granado, C. Kohler, U. Morgner, A. Husakou, and J. Herrmann, Boosting Terahertz Generation in Laser-Field Ionized Gases Using a Sawtooth Wave Shape, Phys. Rev. Lett. **114**, 183901 (2015).

[25] V. A. Kostin, I. D. Laryushin, A. A. Silaev, and N. V. Vvedenskii, Ionization-Induced Multiwave Mixing: Terahertz Generation with Two-Color Laser Pulses of Various Frequency Ratios, Phys. Rev. Lett. **117**, 035003 (2016).

[26] I. Babushkin, S. Skupin, A. Husakou, C. Köhler, E. Cabrera-Granado, L. Bergé, and J. Herrmann, Tailoring terahertz radiation by controlling tunnel photoionization events in gases, New J. Phys. **13**, 123029 (2011).

[27] D. W. Schumacher and P. H. Bucksbaum, Phase dependence of intense-field ionization, Phys. Rev. A **54**, 4271 (1996).

[28] P. B. Corkum, N. H. Burnett, and F. Brunel, Above-Threshold Ionization in the Long-Wavelength Limit, Phys. Rev. Lett. **62**, 1259 (1989).

[29] P. B. Corkum, Plasma Perspective on Strong Field Multiphoton Ionization, Phys. Rev. Lett. **71**, 1994 (1993).

[30] S. C. Rae and K. Burnett, Detailed simulations of plasma-induced spectral blueshifting, Phys. Rev. A **46**, 1084 (1992).

[31] C. Lu, S. Zhang, Y. Yao, S. Xu, T. Jia, J. Ding, and Z. Sun, Effect of two-color laser pulse intensity ratio on intense terahertz generation, RSC Adv. **5**, 1485 (2015).

[32] C. Lu, T. He, L. Zhang, H. Zhang, Y. Yao, S. Li, and S. Zhang, Effect of two-color laser pulse duration on intense terahertz generation at different laser intensities, Phys. Rev. A **92**, 063850 (2015).

[33] M. D. Thomson, V. Blank, and H. G. Roskos, Terahertz white-light pulses from an air plasma photo-induced by incommensurate two-color optical field, Opt. Express **18**, 23173 (2010).

[34] V. A. Andreeva, O. G. Kosareva, N. A. Panov, D. E. Shipilo, P. M. Solyankin, M. N. Esaulkov, P. González de Alaiza Martinez, A. P. Shkuinov, V. A. Markarov, L. Bergé, and S. L. Chin, Ultrabroad Terahertz Spectrum Generation from an Air-Based Filament Plasma, Phys. Rev. Lett. **116**, 063902 (2016).